J. Geodynamics Vol. 15, No. 1/2, pp. 39–58, 1992
Printed in Great Britain.

0264-3707/92 $5.00+0.00

RECENT AND ACTIVE TECTONICS OF THE NORTH-EASTERN ECUADORIAN ANDES

L. FERRARI and A. TIBALDI

Dipartimento di Scienze della Terra, Università di Milano, Via Mangiagalli 34, 20133 Milano, Italy

(Received 4 June 1991)

Abstract—The north-eastern part of the Ecuadorian Andes, comprising the Interandean Valley, the Cordillera Real and part of the Sub-Andean Zone, is a region of diffuse seismicity with events reaching up to Ms = 7.0. The neotectonics of the region east of the Interandean Valley is analysed here by the integration of mesotectonic, microtectonic and seismological data.

The structural setting is characterized by a predominace of N–S and NNE–SSW thrusts in the eastern region; whereas in the western region several NNE–SSW trending right-lateral strike–slip faults are present, the longest of which (the Cayambe–Chingual Fault) has a length of more than 70 km. Right-lateral faults trending NNE–SSW and some oblique thrust faults cut volcanic rocks of Late Pleistocene age and all the other fault sets. These faults offset streams of post-glacial age, are erosionally immature and have triangular facets. These data argue for a recent age for these faults. The Quaternary state of stress computed from microstructural data has a WSW–ENE greatest principal stress which is consistent with published focal mechanism solutions in this region. These consist of a combination of thrusting and right-lateral strike–slip motions along NNE–SSW striking planes. A kinematic model of the upper crust, in which westward dipping oblique thrusts and strike–slip faults coexist and converge at depth, accounts both for the observed seismicity and for the field measurements. These structures are part of a broader fault zone with a predominant right-lateral component of motion which extends along the eastern margin of the Andean Block, from the Gulf of Guayaquil, in southern Ecuador, to northern Colombia.

1. INTRODUCTION

A large earthquake (Ms = 6.9) occurred on 5th March 1987 (local date) in the north-eastern part of the Ecuadorian Andes (Figs 1 and 2), causing hundreds of casualties. An analysis of the catalogue of historical earthquakes reveals that this was not an isolated event, but only the latest expression of diffuse seismic activity.

In spite of this dramatic seismicity and the relatively high density of population of some parts of the Ecuadorian Andes, the available data on the tectonics of the region are insufficient and inadequate. Knowledge of structural features is almost entirely from geophysical studies, including a gravimetric survey on regional crustal structure (Feininger and Seguin, 1983), an analysis of microseismicity (Hall *et al.*, 1980) and studies at a "semi-continental" scale based on teleseismic data (Pennington, 1981; Suarez *et al.*, 1983; Wolters, 1986). The regional structural

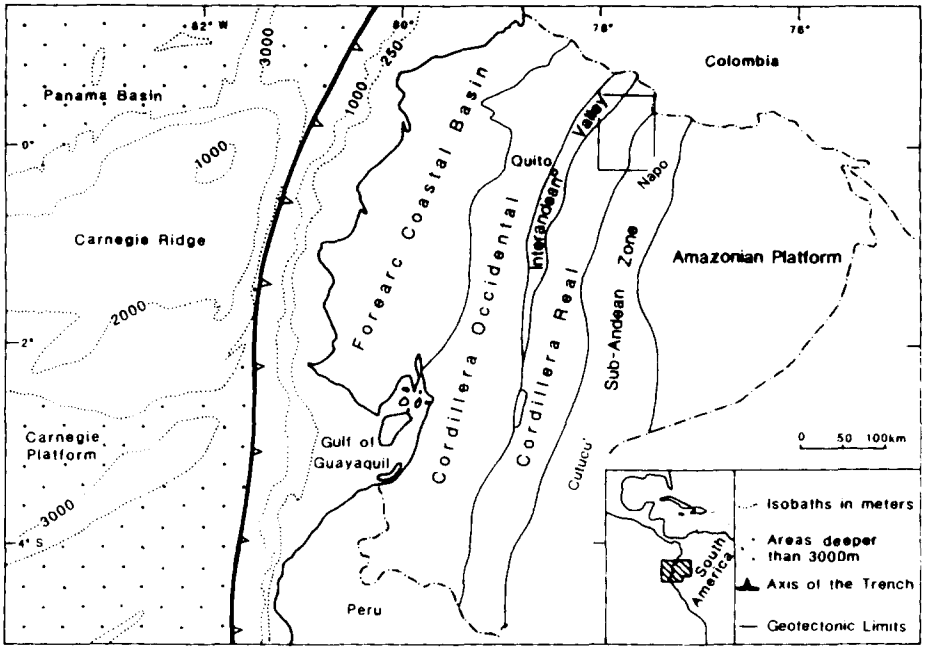

Fig. 1. Sketch map of Ecuador and surrounding areas. The study area is outlined [data from Lonsdale (1978); Lonsdale and Klitgord (1978); Baldock (1982)].

setting has also been inferred from geological reconstructions (Kennerly, 1980; Feininger and Bristow, 1980; Baldock, 1982; Lebras *et al.*, 1987). Some of these authors have inferred a western dextral transcurrent boundary for northern South America, passing through Ecuador between the Cordillera Occidental and the Amazonian Platform. However, such a tectonic feature has never been demonstrated in the field.

In this paper, neotectonic field measurements are integrated with unpublished seismological data, in order to define the relationships between shallow and deep geological structures and the recent and active kinematics of the upper crust. Because the area of study is particularly inaccessible, with steep mountains and dense rainy forest, aerial stereophotos and radar and Landsat MSS images were used, in the initial stage, to plan the field work and the location of the structural stations. The 5th March 1987 earthquake produced a substantial slope denudation which greatly eased the structural field survey. Topographical maps were specially prepared for this study at 1:50,000, 1:75,000, 1:100,000 scales. Geological data were derived from unpublished reports (Barberi *et al.*, 1988; Balseca and Ferraris, 1977).

2. GEOLOGICAL BACKGROUND

Ecuador has three main geographic zones (Fig. 1): a hilly coastal region, a central mountain belt and an eastern Sub-Andean Zone, gently sloping towards the Amazonian Platform. The coastal region is formed by oceanic rocks (ophiolite

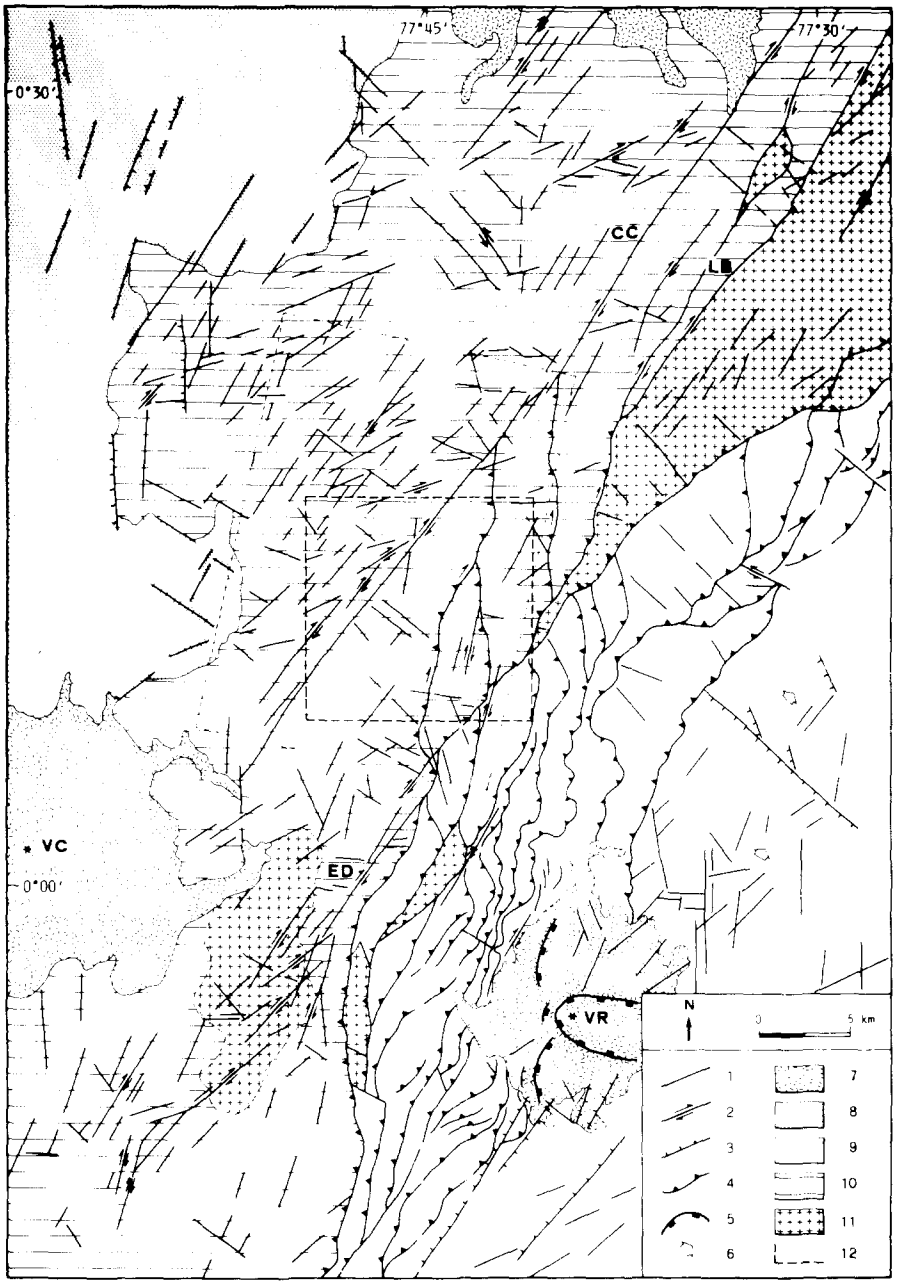

Fig. 2. Structural map derived from Landsat, Radar, aerial and field data. 1, Fault with unrecognized type of motions; 2, strike-slip fault; 3, normal fault; 4, thrust and oblique thrust front; 5, scarp of volcano-tectonic collapse; 6, dip of tilted block; 7, Quaternary volcano; 8, Interandean Valley; 9, Sub Andean Zone; 10, Cordillera Real; 11, outcrop of intrusive rock; 12, area of Fig. 6 (small box) and Fig. 3 (large box). CC = Cayambe-Chingual fault; ED = El Diviso fault; LB 5 La Bonita fault; VC = Volcan Cayambe; VR = Volcan Reventador.

and basalts) and their sedimentary cover of Cretaceous age (Goosens *et al.*, 1977). These rocks are grouped into the Piñon and Cayo Formations. They are partly buried under a thick sequence of Tertiary products filling a series of fore-arc basins (Lonsdale, 1978).

In the central mountain belt two parallel ranges (the Cordillera Occidental and the Cordillera Real) are separated by the narrow Interandean Valley (Fig. 1). The Cordillera Occidental is mainly formed by Cretaceous volcanic rocks with island arc affinity (Macuchi Fm.) (Henderson, 1979; Lebras *et al.*, 1987) covered by discontinuous flysch-like deposits of Cretaceous to Eocene age. As are the coastal Piñon and Cayo Formations the Cordillera Occidental complex is considered an "exotic terrain" accreted onto the South American margin probably in Early Tertiary time (Feininger and Bristow, 1980; Lebras *et al.*, 1987; Roperch *et al.*, 1987). In this framework, the Interandean Valley is a suture between the island arc and the continental paleomargin.

The Cordillera Real is part of a metamorphic belt that runs continuously from Colombia to the Peruvian border. Although the geology of the Cordillera Real is poorly known, distinct metamorphic associations have been recognized. The oldest core of this range outcrops in its northern part and is formed by migmatites, orthogneisses and quartz-feldspathic amphibolites known as the Cofanes Group (Baldock, 1982). These rocks are considered to be Precambrian in age, by correlation with similar complexes in southern Columbia (Directiòn General de Geologìa y Minas, 1986). Lower grade metamorphic rocks, generally in Barrovain facies, are present in the Ambuquí and Llangantes Groups, which outcrop to the west and to the south. These units are attributed to the Paleozoic (Baldock, 1982) and can be followed northward into Colombia (Feininger, 1982; McCourt *et al.*, 1984). The Cordillera Real has undergone several orogenic phases since the Cretaceous and probably since Paleozoic times (Zeil, 1979). The Andean orogenesis, due to the accretion of old Pacific plates and subduction of the Nazca Plate under the South American Plate, produced an overlapping of the Cordillera Real units onto the Sub-Andean zone along several WNW dipping thrust planes.

The upper Paleozoic to Mesozoic volcanic and sedimentary formations outcropping in the Sub-Andean Zone are the cover of the Precambrian Guyana shield (Feininger, 1982). In the area studied they include the volcanic Misahuallí Formation, the terrigeneous and carbonatic Hollín and Napo formations and the molasse-type Tena formations. These units of Jurassic–Paleocene age (Baldock, 1982) are involved in the structural dome of the Napo uplift. The Sub-Andean Zone is an extension of a fold-thrust belt which has developed in response to a still active orogenic pulse that began in the Late Miocene. Several granodioritic batholiths crop out along the boundary between the Cordillera Real and the Sub-Andean Zone. They form a belt of elongated plutonic bodies of possibly Jurassic age that can be followed northwards into Colombia.

Continental volcanism began in the late Miocene and is widespread in the Interandean Valley, but there is no Quaternary activity south of Lat. 2 S (Barberi

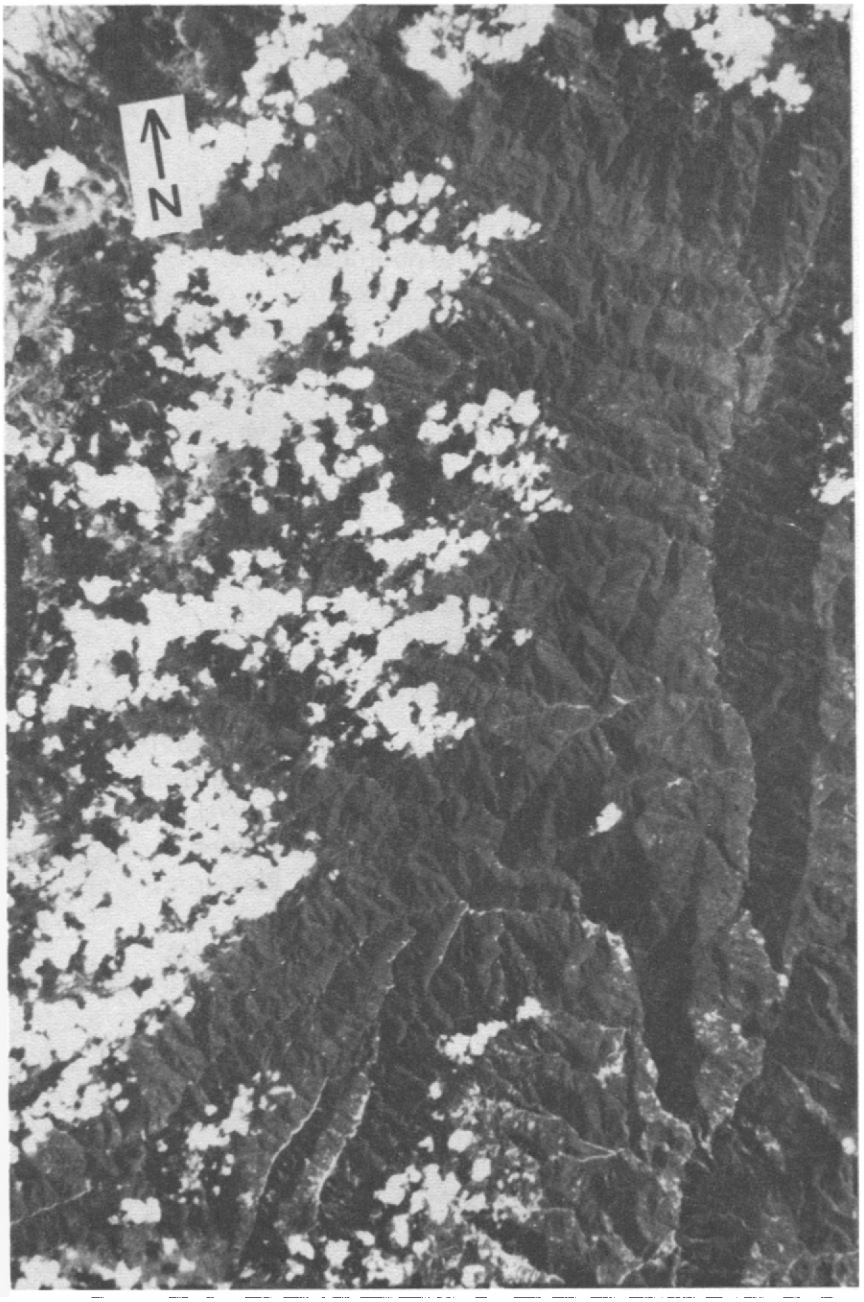

Fig. 3. Enlargement of Landsat MSS band 7 image. Largest side is 42.5 km long. The NNE–SSW CC Fault is clearly recognizable (original image at 1:250,000 scale).

et al., 1988b). The volcanic arc reaches its maximum width in the northern part of the country, where some stratovolcanoes are present in the Sub-Andean Zone (e.g. the Quaternary Reventador Volcano).

3. TECTONICS

3.1. Structural features

The area studied is mainly in the Cordillera Real. The high mountains are largely dissected by fluvial and glacial erosion. For this reason the structural map of Fig. 2 was made integrating field and photogeological data. The outstanding feature of this area is a family of linear faults with an overall trend of N 30. The Cayambe–Chingual fault (CC) is clearly visible on a satellite image (Fig. 3). It extends for more than 70 km from north of the Cayambe volcano to the northeast into Colombia. Field analyses of slickenside fault surfaces revealed that the motions were of right-lateral strike–slip type. Two other large strike–slip faults, El Diviso (ED) and La Bonita (LB), parallel the CC to the east. The latter is connected with the ED by two thrust faults with westward dip. Another thrust is bounded to north by the LB. Taken as a whole, these structures define an oblique transpressive zone named the El Dorado Duplex System (Fig. 4). Close to the principal structures secondary systems of strike–slip faults have three main trends: N40-55, N15-25 and N135.

Toward the east, a widespread zone of westward dipping thrusts bring into contact intrusive and metamorphic rocks of the Cordillera Real with volcanic and sedimentary rocks of the Sub-Andean Zone. The western sector of the Sub-Andean Zone shows thrusts with a smaller amount of displacement which extend eastward to Reventador Volcano (Fig. 2). Further to the east, deformation diminishes in intensity. The area contains a series of titled blocks and a few open folds, then passes gradually to the Amazonian Platform.

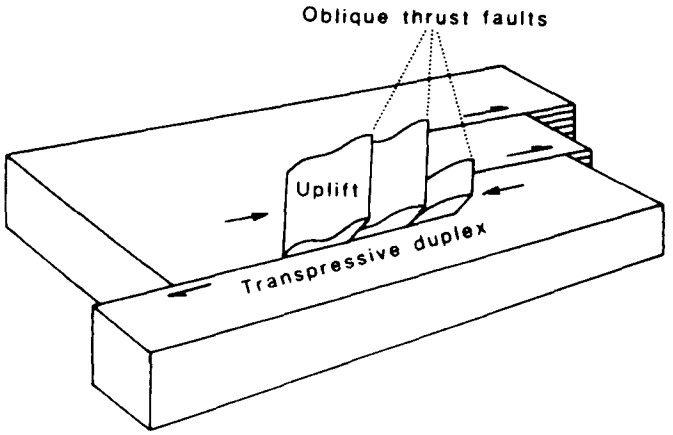

Fig. 4. Schematic diagram showing the structure of the El Dorado Duplex System.

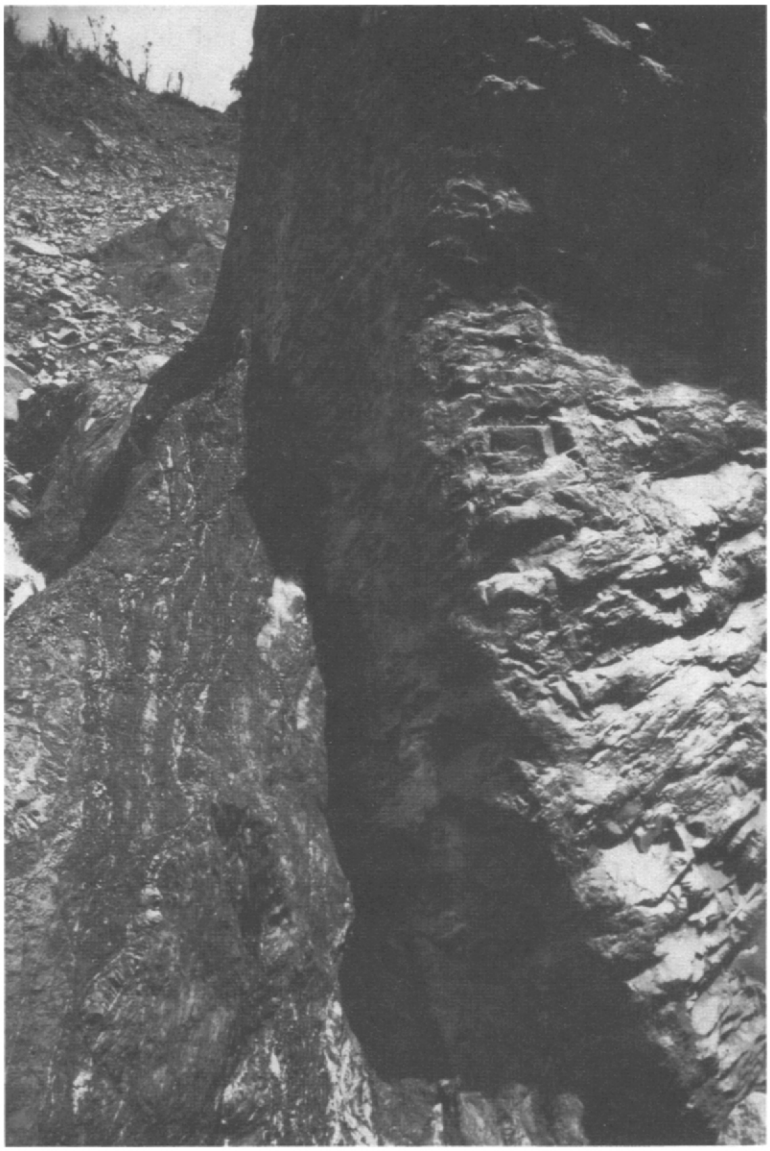

Fig. 5. A NNE–SSW right-lateral strike-slip fault (the vertical plane in the middle of the frame) displaces a Late Pleistocene volcanic dome (right) located on the western slope of Reventador Volcano. The part of the dome shown in the picture is 3 m wide approximately.

3.2. *Neotectonic indicators*

The NNE–SSW right-lateral strike–slip faults displace all rock units dating up to the Late Pleistocene. This is evident in the dome built on the western flank of Reventador Volcano (whose base is dated 0.3 Ma). The volcano is cut by a transcurrent fault of the NNE–SSW set (Fig. 5). In contrast the NNE–SSW reverse faults do not cut these volcanic products and thus belong to an older phase (Fig. 6). Other Pliocene–Quaternary deposits are lacking but, even so, two tectonic phases preceded the transcurrent phase and can be recognized after the Oligocene. A major phase of thrusting took place during the Miocene (Baldock, 1982), and was followed by a second phase of right-lateral thrusting deformations (Pasquarè *et al.*, 1990). Thus, within the Pliocene–Quaternary time span, it seems resonable to assign a Pliocene age to the oblique thrust phase and a Quaternary age to the transcurrent phase. Most of the NNE–SSW rectilinear faults are erosionally immature and exert a small control on the drainage network. This has proved to be a fairly good indicator of recent faulting (Marino and Tibaldi, 1989, 1990). Moreover, the uniform sense of displacement of the drainage pattern shown by some of these faults, (e.g. CC, Fig. 7), is a very important neotectonic indicator as pointed out by Peizhen *et al.*, (1988). The rivers dissect a glacial morphology, so we infer that fault motions occurred also after the last glacial phase [20,000 years, Clapperton and Vera (1986)]. Finally, triangular facets are widespread along the NNE–SSW fault set.

Fig. 6. Low angle thrust planes displacing Cenozoic units. The photo has been taken along the Rio Malo (3 km west of Reventador Volcano).

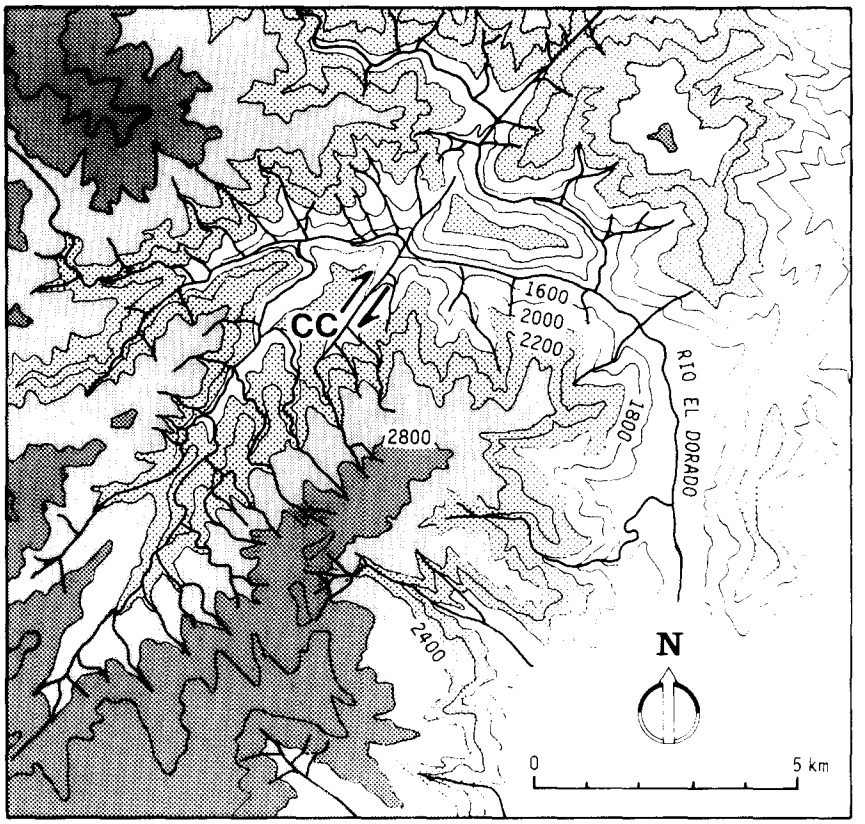

Fig. 7. Topography of part of the CC Fault. Note the turning of the tributaries for drag effects along the fault trace. The distortion of the hydrographic pattern confirms the Quaternary right-lateral strike-slip motions detected on the slickenside fault planes.

Where the NNE–SSW transcurrent faults intersect E–W and WNW–ESE left-lateral strike-slip faults, the two sets displace each other. We consider these sets conjugated.

3.3. Stress field

Striations from Quarternary fault planes were processed in order to calculate a state of stress. We used a computer program based on Carey's algorithm (Carey, 1976, 1979). The method is based on the assumption of Bott (1959) that slip along the fault plane takes place in the same direction and sense as the maximum shear stress acting on this plane. The computed stress directions obtained at 26 structural sites are shown in Fig. 8 and partly on the stereographic projections of Fig. 9 while the stress tensor parameters are presented in Table 1. The computed stress field (Fig. 10) trends WSW–ENE for the greatest principal stress (σ_1). In the Sub-Andean Zone a change of the tensor shape produced the inactivation of the easternmost thrusts and the local development of normal

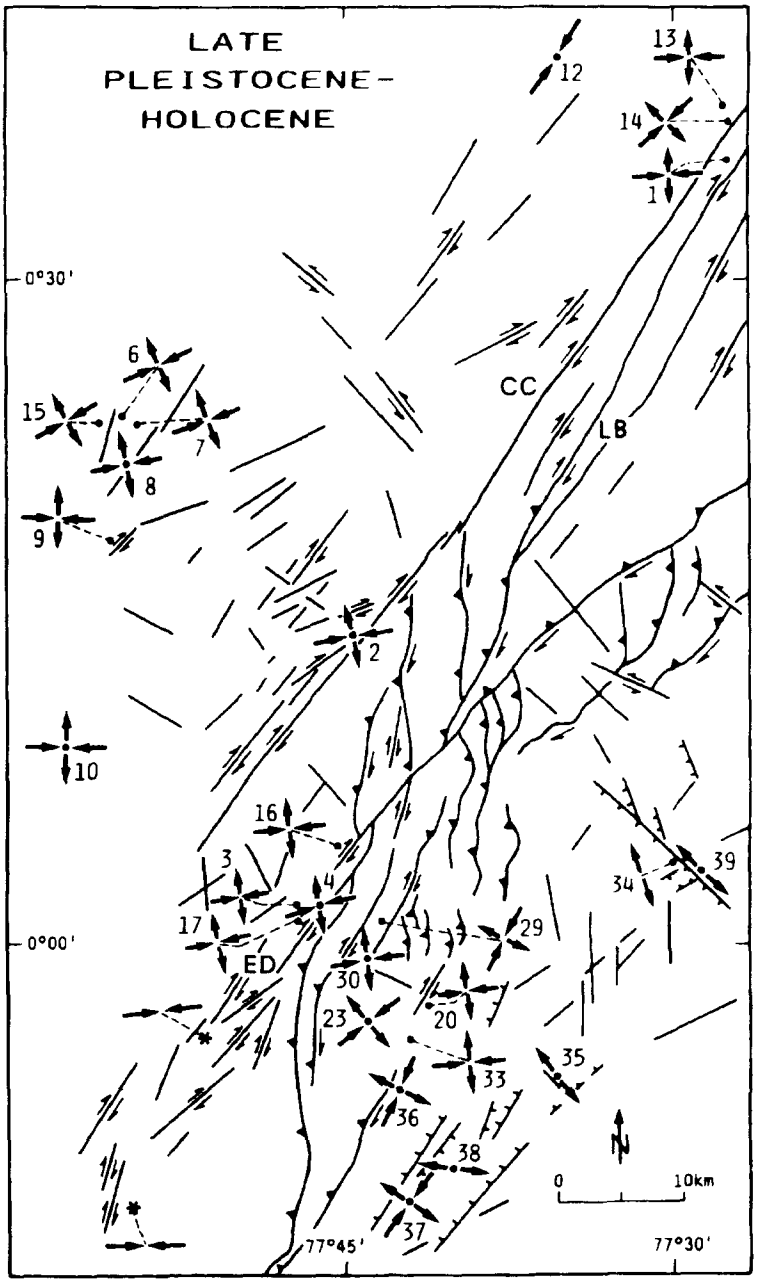

Fig. 8. Tectonics and state of stress during the Quaternary. The map shows active faults, directions of principal stresses and deformation mechanisms. Converging arrows indicate the direction of greatest principal stress (σ_1), diverging arrows that of least principal stress (σ_3). Numbers refer to location of structural sites. See Table 1 for computed stress tensor. Asterisks without numbers refer to the epicenters of 5th March 1987 earthquakes with arrows representing the P axes.

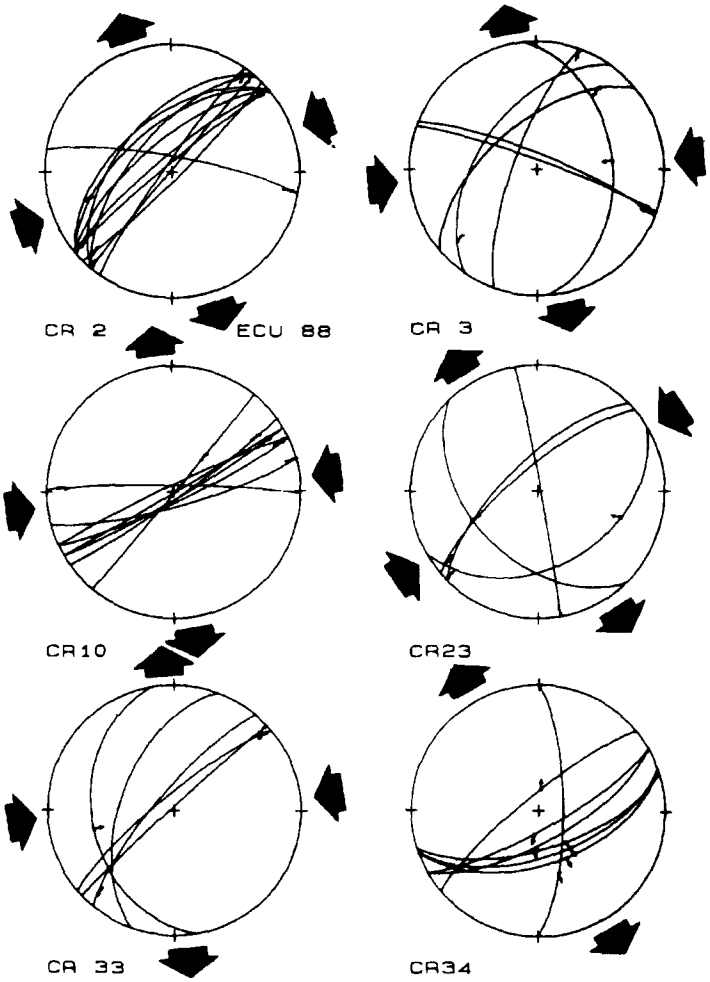

Fig. 9. Selected stereograms from structural stations used to compute solutions for Quaternary state of stress. Schmidt projection, lower hemisphere. Numbers of stations as in Fig. 8. See Table 1 for parameters of stress tensor.

faults. This type of kinematics can be explained by an interchange between σ_1 and σ_2. They allowed volcanic activity to be established.

3.4. Seismological data

We have described a large number of faults, mainly striking NNE–SSW which have been active in Quaternary times in the north-eastern Ecuadorian Andes. These data are compatible with the distribution of the shallow seismicity at a larger scale (Fig. 11). The 93 collected events come from the catalogues of the NOAA, CERESIS (1986) and Observatorio Astronomico de Quito (1981) for the years 1903–1987 A.D. Because of the distribution of recording stations of the international network, the catalogues are incomplete for events with Ms< 5 in this area. Nevertheless a high level of seismicity is concentrated along the

Table 1. Parameters of the deviatoric stress tensor computed from the Quaternary faults of the northern Cordillera Real

			Principal stress direction							
			σ_1		σ_2		σ_3		Shape factor	
Site	NF	Long. Lat.	Azim.	Dip	Azim.	Dip	Azim.	Dip	$R(e)$	$R(a)$
CR 1	5	77°29′ 0°37′ N	261	1	165	71	351	18	0.29	0.29
CR 2	11	77°45′ 0°14′ N	70	3	333	67	162	21	0.16	0.16
CR 3	6	77°47′ 0°02′ N	85	14	254	75	354	3	0.30	0.30
CR 4	5	77°46′ 0°02′ N	258	5	86	85	348	1	0.85	0.85
CR 6	5	77°55′ 0°24′ N	55	16	219	73	322	4	0.47	0.47
CR 7	8	77°54′ 0°19′ N	250	14	31	71	156	10	0.47	0.47
CR 9	6	77°57′ 0°09′ N	95	6	261	83	6	1	0.37	0.37
CR10	8	77°30′ 0°40′ N	84	14	253	75	353	3	0.23	0.23
CR13	7	77°29′ 0°38′ N	86	12	305	74	179	9	0.07	0.07
CR14	6	77°56′ 0°23′ N	226	7	91	79	317	7	0.30	0.30
CR15	6	77°46′ 0°13′ N	236	7	352	72	144	15	0.32	0.32
CR16	6	77°42′ 0°02′ S	254	5	92	84	344	1	0.04	0.04
CR20	11	77°47′ 0°04′ S	79	2	343	76	170	13	0.33	0.33
CR23	5	77°44′ 0°01′ N	239	1	330	29	148	69	0.02	0.02
CR29	6	77°44′ 0°01′ N	35	6	286	71	126	16	0.77	0.77
CR30	5	77°44′ 0°00′	253	8	42	80	160	4	0.82	0.82
CR33	5	77°43′ 0°04′ S	83	9	314	75	175	11	0.53	0.53
CR34	7	77°31′ 0°04′ N	195	79	62	7	330	8	2.90	0.34
CR35	5	77°36′ 0°07′ S	292	80	57	6	148	8	2.27	0.47
CR36	6	77°42′ 0°07′ S	35	8	261	78	123	9	0.32	0.32
CR37	8	77°41′ 0°08′ S	43	16	214	74	312	3	0.54	0.54
CR39	6	77°30′ 0°04′ N	207	81	44	8	314	3	45.01	0.02

Sites are numbered as in Fig. 7. NF is the number of the fault planes used in computing the solutions. In each station 100% of the observed slip vectors show less than 150 of deviations from the predicted ones. Azimuths are measured clockwise from north; dip is toward the measured azimuth. $R(e) = (\sigma_2-\sigma_3)/(\sigma_1-\sigma_3)$; its value varies between $+\infty$ to $-\infty$; $R(a) = (\sigma_2-\sigma_3)/(\sigma_1-\sigma_3)$; its value varies between 0 and 1.

NNE–SSW Interandean Valley and the Cordillera Real. A number of historical events during the period 1561–1905 A.D. have also been reported in this area. Seven large earthquakes (estimated intensity of Mercalli scale IX) occurred in the area of Fig. 11 (Observatorio de Astronomico Quito, 1959). These data demonstrate tectonic movements along the eastern zone of the northern Ecuadorian Andes, including the Interandean Valley, the Cordillera Real and, at a lower level, the Sub-Andean Zone. The western Andes (i.e. Cordillera Occidental), in contrast show lower levels of crustal tectonic activity (Barberi *et al.*, 1988a; Pasquarè *et al.*, 1990).

The epicenters of the two large events that occurred on 5th March 1987 (b and c in Fig. 11) show a NNE–SSW alignment, coincident with the orientation of Quaternary faults recognized in the field. A similar alignment is shown by the microseismicity recorded during the periods January–April 1981 (1 in Fig. 11) and December 1986–March 1987 (2 and 3 in Fig. 11) (Barberi *et al.*, 1988a).

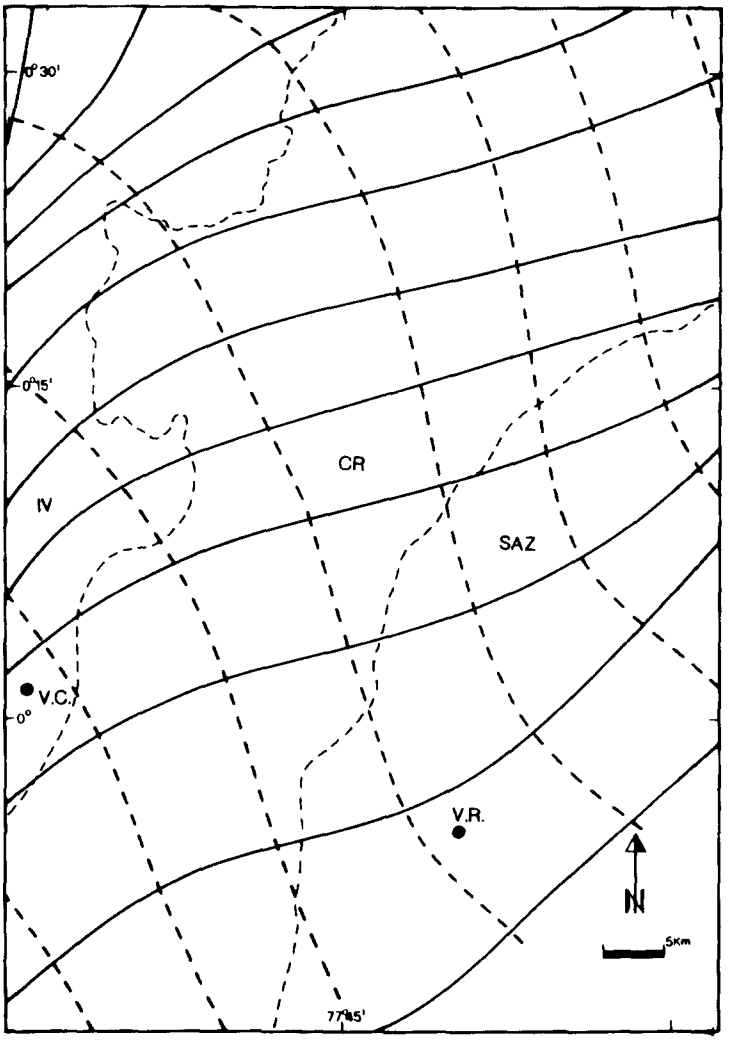

Fig. 10. Quaternary stress field map computed from the data presented in this work. Continuous and dashed lines show average traiectories of σ_{Hmax} and σ_{Hmin} respectively.

The focal mechanisms of some of these events have been published and are shown in Fig. 11 (data in Table 2). The events of 5 March 1987 (USGS, 1987) show a dominant thrust motion with a right-lateral strike-slip component (b and c Fig. 11). Centroid Moment Tensor solutions for the same events (Dziewonski *et al.*, 1988) show nearly pure thrust motions but very similar *P* and *T* axes (Table 2). The event of 5 August 1949 (Woodward & Clyde, 1981) (e in Fig. 11) shows almost pure transcurrent motions along NE–SW striking plane. The NNE–SSW and NE–SW nodal planes were assumed to be the fault planes because all the major faults of the area have the same orientation. All these solutions agree quite well with the microtectonic analyses. The 390 motion vectors collected

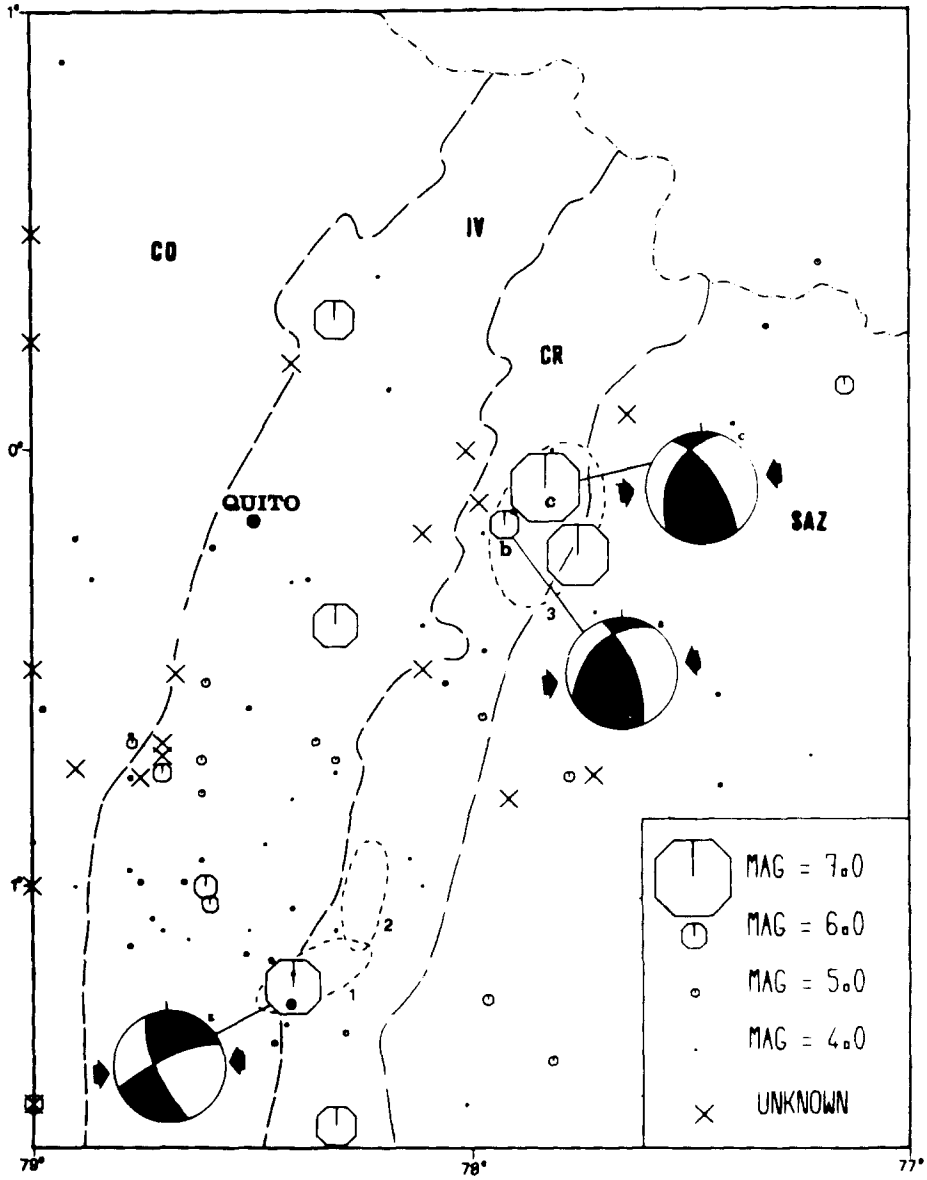

Fig. 11. Epicenter distribution map. CO, Cordillera Occidental; IV, Interandean Valley; CR, Cordillera Real; SAZ, Sub-Andean Zone. Numbers 1, 2 and 3 refer to microseismicity analysis discussed in the text. Letters refer to focal mechanisms: after Woodward & Clyde (1981), b and c after Barberi *et al.* (1988a); black arrows show horizontal direction of *P* axis; Schmidt projection, lower hemisphere.

on the Quaternary slickensided fault planes show predominant right-lateral strike–slip motions along NNE–SSW main faults, with subsidiary thrust components.

The isoseismal map of the event of 5th March 1987 shows a clear NNE–SSW elongation (Fig. 12). Since the isoseismal shape depends on the hypocentral depth of the related event and on geological structures such as basins, it cannot be directly linked to the trend of the seismogenetic structure (Panza *et al.*, 1992).

Table 2. Parameters of the earthquakes discussed in the text

Date	Time	Lat.	Long.	Depth (km)	Ms	*T* axis		*P* axis		Method	Source
						Tr.	Pl.	Tr.	Pl.		
A 5 Aug ,1949	19:08:55	−1.23S	−78.40W	45	6.7	39	53	265	46	CFM	1
B 6 Mar, 1987	01:54:57	0.10N	−77.65W	14	6.1	218	50	102	21	MTS	3
B 6 Mar, 1987	01:54:49	0.05N	−77.65W	14	6.1	218	50	102	21	MTS	3
C 6 Mar, 1987	04:10:55	−0.06S	−77.84W	15	6.9	268	71	100	19	CMT	2
C 6 Mar, 1987	04:10:42	0.15N	−77.82W	49	6.9	196	52	82	17	MTS	3

CFM = Composite Focal Mechanism; CMT = Centroid Moment Tensor; MTS = Moment Tensor Solution; 1, Woodward & Clyde (1981); 2, U.S.G.S. (1987); 3, Dziewonski *et al.* (1988).

Even so, as all the major structures of the area strike NNE–SSW, the isoseismals elongation seems to correlate with fault strike.

A more detailed picture of macroseismicity is revealed by the distribution of the landslides triggered by the March 5 1987 earthquakes (Cavallin *et al.*, 1989) (Fig. 12). Although the amount of landslides resulted to be fairly well correlated with the lithology and the acclivity, those factors have an influence only on a small scale, so that the general pattern may be reasonable comparable to an isoseismal map. On this map the effects of the earthquakes are observable along a wide zone elongated in a NNE–SSW direction for about 70 km. Such a length is comparable with the fault rupture length expected from the magnitude of the events according to the curves of Slemmons (1977).

4. DISCUSSION AND CONCLUSIONS

Field observations carried out in the northern Ecuadorian Andes have demonstrated Quaternary tectonic activity in the eastern belt, which includes the Interandean Valley, the Cordillera Real and the westernmost part of the Sub-Andean Zone. These data are consistent with the recorded seismic activity of the Ecuadorian Andes, which is concentrated in its eastern part and is very scarce in the Cordillera Occidental.

The relatively low level of seismicity in the western Sub-Andean Zone seems to contradict the neotectonic field evidence. However, the seismic data set is quite poor both for low magnitude and for historic events. According to field observations, Quaternary motions took place along major NNE–SSW and N–S faults and some rare secondary NW–SE faults. The most developed faults of the area trend NNE–SSW. Among them is the 70 km-long CC Fault. This fault partly coincides with a lineament published in the Baldock map (1982), but is recognized here as a Quaternary and active master fault. The two large events of 5 March 1987 and the recorded microseismicity also define a NNE–SSW trend (Fig. 11). The same orientation is shown by the isoseismal map of those events (Fig. 12), based on surface damage and on landslide distribution.

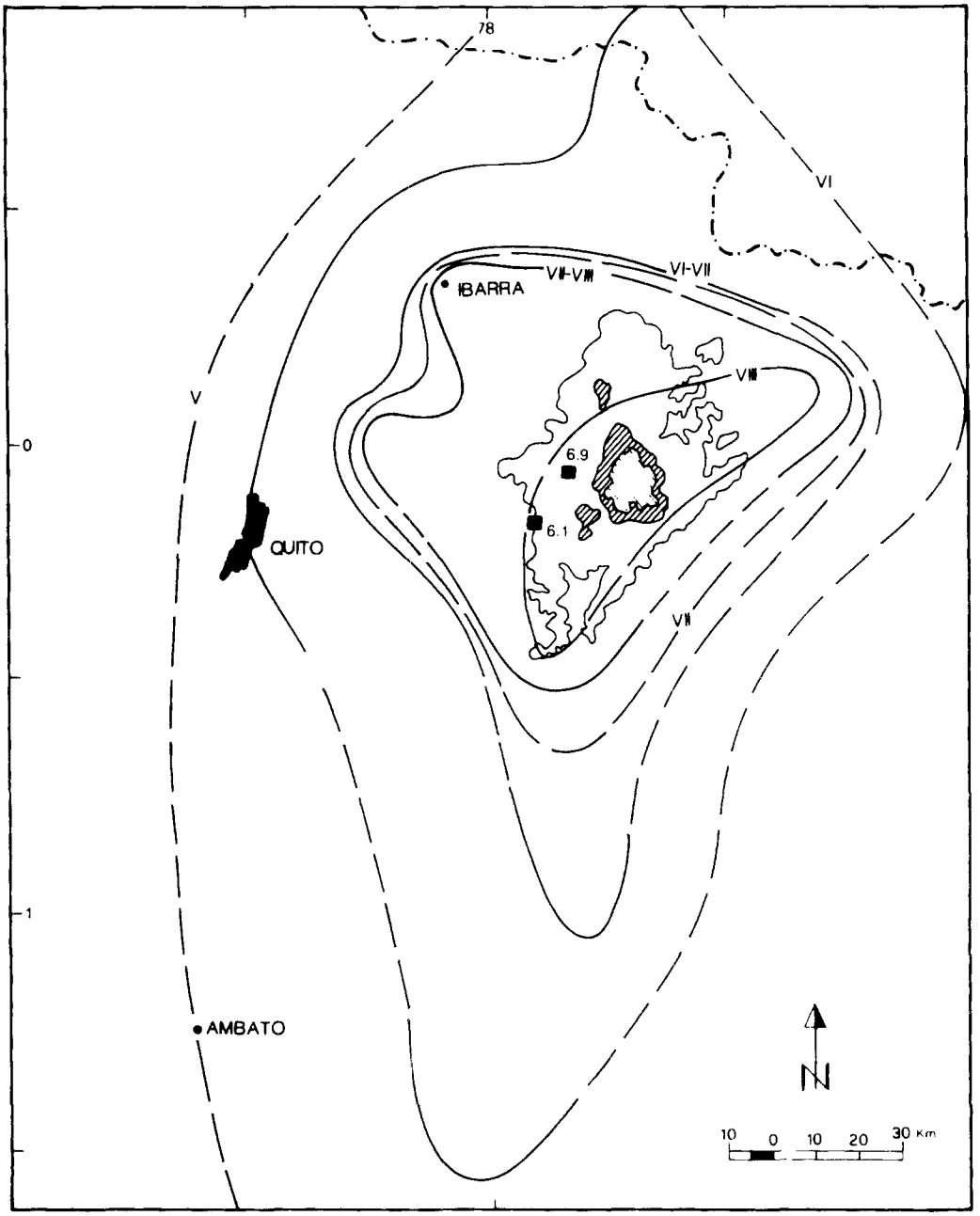

Fig. 12. Isoseismal map of the 5th March 1987 earthquake [after Barberi *et al.* (1988a)]. The intensity (Mercalli scale) is indicated for each line. Boxes represent the two main shocks epicenters with magnitude. Smaller areas within sinuous lines represent percentage of landslide area for this seismic events (white = 1–30%, heavy lines = 31–6%, light lines 60%) [data after Cavallin *et al.* (1989)].

The Cayambe–Chingual Fault and the parallel swarm underwent right-lateral strike–slip motions, while the secondary NW–SE faults underwent left-lateral strike–slip motions. In addition, a thrust component has been recognized on N–S en echelon faults as well as on some other NNE–SSW faults. This right-lateral thrusting is also revealed by the focal mechanisms of the 5 March 1987 events (Fig. 11).

By combining the Quaternary orientations of principal stresses, obtained from microtectonic analyses, with the direction of the *P* axes of focal mechanisms, it is possible to calculate the stress field in the shallow crust (Fig. 10). The north-eastern Andes are subject to a regional ENE–WSW horizontal greatest principal stress(σ_{Hmax}). In the Cordillera Real this stress is coincident with σ_1. The regional horizontal least principal stress (σ_{Hmin}) is oriented NNW–SSE and is coincident with σ_3 or σ_2 depending on whether strike–slip or thrust motion is predominant.

These data are useful for evaluating the geometry and kinematics of the principal tectonic units. The upper crustal units are bounded by sectors of the Cordillera Real moving toward the NNE along major NNE–SSW right-lateral strike–slip faults (S in Fig. 13). They mostly dip toward the WNW at high angles. Alternatively, the regional stress can induce strike–slip motions with a variable thrust component along faults dipping toward the WNW at a lower angle (T in Fig. 13). N–S en enchelon faults can be activated with a predominant thrust component (E in Fig. 13). We suggest that the N–S en echelon faults converge at depth in NNE–SSW striking planes. This implies contemporaneous strike–slip and oblique thrust deformations. Such a partitioning of the motion has been observed both in

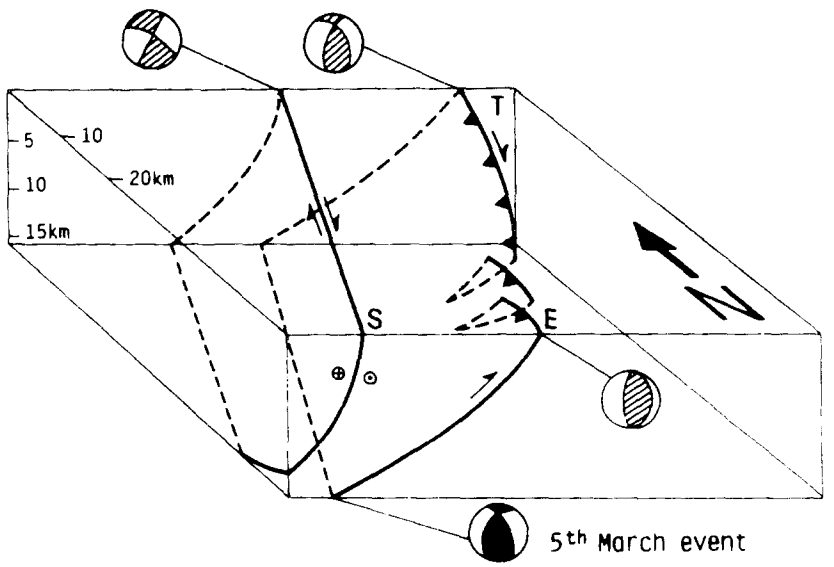

Fig. 13. Schematic three-dimensional model of Late Pleistocene–Holocene faulting in the northern Cordillera Real. Focal mechanisms with shaded areas represent theoretical types of motions which could develop along NNE–SSW and N–S faults as inferred from structural field observations. S, Right-lateral strike–slip faults; T, right-lateral strike–slip faults with a thrust component; E, en echelon faults with predominant thrust component.

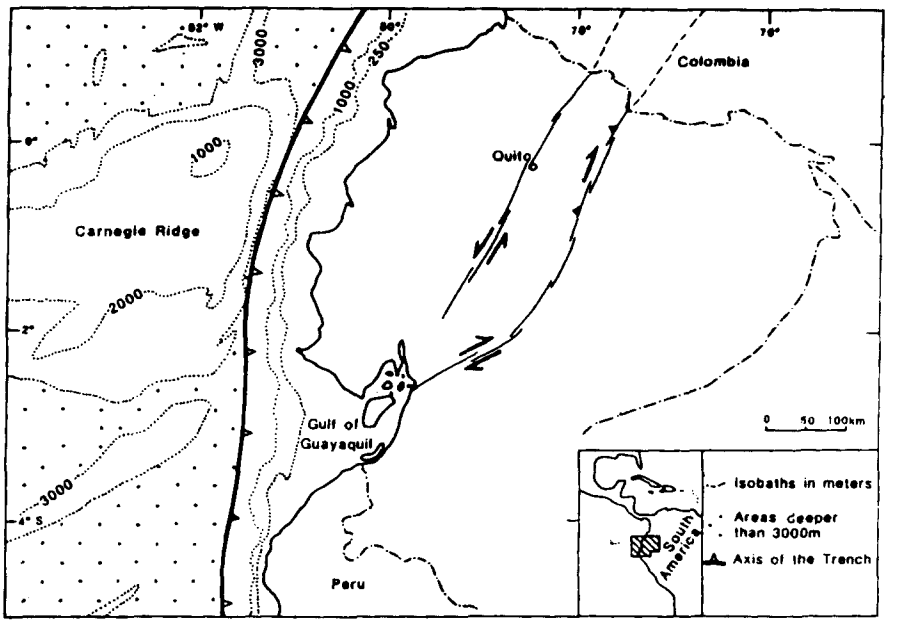

Fig. 14. Major Quaternary tectonic features of Ecuador and surrounding areas, according to the results of this study and Tibaldi and Ferrari (1992).

experimental models and in other areas of the world (Abers and McCaffrey, 1988; Tapponnier *et al.*, 1989; Richard and Cobbold, 1989).

Finally, these structures can be correlated with the Pallatanga fault system (Winter and Lavenu, 1989) and with the fault zone of the east Andean front of Colombia (Pennington, 1981). The data presented in this work provide field evidence for the right-lateral Quaternary character of this large fault zone bounding the Andean Block. Other large strike–slip Quaternary motions have been recognized in the Interandean Valley (Tibaldi and Ferrari, 1992) providing further insights into the transcurrent fragmentation of the Andean Block (Fig. 14).

Acknowledgements—This work was largely carried out in the frame of a contract between the University of Milan and ELC- Electroconsult Society, Milan, Italy. Field work by A.T. benefited also of a Ph.D. grant from Ministero Italiano della Pubblica Istruzione. We are indebted to W. Balseca, M. Ferraris and G. Pasquarè for field assistance and G. Zonno for useful discussions. We wish to thank R. Cassinis for critically reading the manuscript and P. Cobbold for the peer review of the work. D. Agalbato provided the earthquake catalogues and A. Ranzoni kindly assisted us in drawing the epicenter distribution map. INECEL- Quito supplied helicopter and logistic facilities. RODIO provided accommodation in a jungle camp.

REFERENCES

Abers G. and McCaffrey R. (1988) Active deformation in the New Guinea fold-and-thrust belt: seismological evidence for strike–slip faulting and basement-involved thrusting. *J. Geophys. Res.* **93**, 332–354.

Baldock, J. W. (1982) Geologìa del Ecuador. Boletín de la explicación del Mapa Geològico de la Republica del Equador, escala 1:1.000.000. *Dirección General de Geologìa y Minas*, Quito, Ecuador.

Balseca W. and Ferraris M. (1987) Informes geologìco sobre el volcàn Reventador. *Tech. Repts. Coca-Codo Sinclair Proj., INECEL, Quito.*

Barberi F., Belloni L., Ferrari L., Pasquare' G., Previtali F., Tibaldi A. and Zonno G. (1988a) Riesgo sismico. *Tech. Rpt. Coca-Codo Sinclair Proj., Quito.*

Barberi F., Coltelli M., Ferrara G., Innocenti F., Navarro J. M. and Santacroce R. (1988b) Plio-Quaternary volcanism in Ecuador. *Geol. Mag.* **125(1),** 1–14.

Bott M. H. P. (1959) The mechanisms of oblique slip faulting. *Geol. Mag.* **96,** 109–117.

Cavallin A., Ferrari L., Pasquarè G., Slejko D. and Tibaldi A. (1989) Landslides and debris-flows triggered by the 1987 earthquake in the Reventador area (Ecuador). *Proc. 2nd Int. Conf. geomorphology*, 3–9 September Frankfurt, RDT. Geoöko-plus, Vol. 1, pp. 50–51 (abstract).

Carey E. (1976) Analyse numérique d'un modèle mécanique élémentaire appliqué à l'étude d'une population de failles: Calcul d'un tenseur moyen des contraintes à partir des stries de glissement. Ph.D. Thesis, Univ. Paris-Sud, Orsay.

Carey E. (1979) Recherche des directions principales de contraintes associées au jeu d'une population des failles. *Rev. Geogr. Phys. Geol. Dyn.* **21(1),** 57–66.

CERESIS (1986) Catàlogo de terremotos para Amèrica del Sur. Datos de hipocentros e intensidades. Quito.

Clapperton C. M. and Vera R. (1986) The Quaternary glacial sequence in Ecuador: a reinterpretation of the work of Walter Sauer. *J. Quater. Sci.* **1,** 45–56.

Direcciòn General de Geologia y Minas, Quito (1986) Mapa geologico "S. Gabriel"; 1:100.000 scale.

Dziewonski A. M., Ekström G., Woodhouse J. H. and Zwart G. (1988) Centroid moment tensor solutions for January–March, 1987. *Phys. Earth Planet. Int.* **50,** 116–126.

Feininger T. (1982) The metamorphic "basement" of Ecuador. *Geol. Soc. Am. Bull.* **93,** 87–92.

Feininger T. and Bristow C. R. (1980) Cretaceous and Paleogene geologic history of coastal Ecuador. *Geol. Rundschau* **69,** 849–874.

Feininger T. and Seguin M. K. (1983) Simple Bouguer gravity anomaly field and the inferred crustal structure of continental Ecuador. *Geology* **11,** 40–44.

Goosens P. J., Rose W. I. and Flores F. (1977) Geochemistry of tholeites of the Basic Igneous Complex of northwestern South America. *Geol. Soc. Am. Bull.* **88,** 1711–1720.

Hall M. L., Basabe P. and Yepes H. (1980) Estudio de las fallas tectonicas y la actividad microsismica del Valle Interandino entre Pastocalle y Ambato. *Politecnica, Monofrafia de Geol.* **V,** 57–78.

Henderson W. G. (1979) Cretaceous to Eocene volcanic arc activity in the Andes of nothern Ecuador. *J. Geol. Soc., London* **136,** 367–378.

Kennerly J. B. (1980) Outline of the geology of Ecuador. *Overseas Geol. Miner. Resourc.*, No. 55.

Lebras M., Megard F., Dupuy C. and Dostal J. (1987) Geochemistry and tectonic setting of pre-collision Cretaceous and Paleogene volcanic rocks of Ecuador. *Geol. Soc. Am. Bull.* **99,** 569–578.

Lonsdale P. (1978) Ecuadorian subduction system. *AAPG Bull.* **62,** 2454–2477.

Lonsdale P. and Klitgord K. D. (1978) Structure and tectonic history of the eastern Panama basin. *Geol. Soc. Am. Bull.* **89,** 981–999.

Marino C. M. and Tibaldi A. (1988) Cronologia tettonica relativa mediante quantificazione del controllo strutturale sul reticolato idrografico telerilevato. *Istituto Lombardo di Sci. Let. Minalo, B* **122,** 293–315.

Marino C. M. and Tibaldi A. (1989) Examples of possible relationships between the hydrographic network as revealed by Landsat images and the tectonic chronology in the Algerian and Tunisian Atlas. *Proc. 28th Int. Cong. Geol. Washington DC, (abstract),* **2,** 368.

McCourt W. J., Aspden J. A. and Brook M. (1984) New geological and geochronological data from the Colombian Andes: continental growth by multiple accretion. *J. Geol. Soc. London* **141,** 831–845.

Observatorio Astronomico de Quito (1959) Breve historia de los principales terremotos de la Republica del Equador. Publicacion del Comite' del Ano Geofisico Internacional de Ecuador, Quito Ecuador.

Observatorio Astronomico de Quito (1981) *Catalogo de Sismos del Ecuador, 1990–1980.*

Panza G. F., Craglietto A. and Suhadolc P. (1992) Source geometry of historical events retrieved by synthetic isoseismals. *Tectonophysics* (in press).

Pasquarè G., Tibaldi A. and Ferrari L. (1990) Relationships between plate convergence and tectonic evolution in the Ecuadorian active thrust belt. In: *Critical Aspects of Plate Tectonic Theory* Augusthitis, S. S. (ed.), pp. 365–387. Theophrastus Publications, Athens.

Pennington W. D. (1981) Subduction of the Eastern Panama Basin and seismotectonics of North Western South America. *J. Geophys. Res.* **86,** 10753–10770.

Peizhen Z., Molnar P., Burchfiel B. C., Royden L., Yipeng W., Qidong D., Fangmin S., Weiqi Z. and Decheng J. (1988) Bounds on the Holocene slip rate of the Haiyuan Fault, North Central China. *Quaternary Res.* **30,** 151–164.

Richard P. and Cobbold P. R. (1990) Experimental insights into partitioning of fault motions in continental convergent wrench zones. *Annls Tectonicae* **4,** 35–44.

Roperch P., Megard F., Laj C., Mourier T., Clube T. M. and Noblet C. (1987) Rotated oceanic blocks in western Ecuador. *Geophys. Res. Lett.* **14,** 558–561.

Slemmons D. B. (1977) Faults and earthquake magnitude. U.S. Army Congress of Engineers, Waterways Experimental Stations. Miscellaneous Papers S 73-1, Reprint 6, 1–129.

Suarez G., Molnar P. and Burchfiel B. C. (1983) Seismicity, fault plane solutions, depth of faulting, and active tectonics of the Andes of Peru, Ecuador and Southern Colombia. *J. Geophys. Res.* **88,** 10403–10428.

Tapponnier P., Armijo R. and Lacassin R. (1989) Fault bifurcation and partition of strike- and dip-slip at mechanical interfaces in the continental lithosphere. *Int. Workshop on Active Recent Strike-Slip Tectonics*, Florence, Italy, (Abstract), 30.

Tibaldi A. and Ferrari L. (1992) From latest Miocene thrusting to Quaternary transpression and transtension in the Interandean Valley, Ecuador. *J. Geodynamics* **15,** 59–83.

U.S.G.S. (1987) Preliminary determination of epicenters (PDE). Monthly listing, March 1987. U.S. Dept. of the Interior.

Winter T. and Lavenu A. (1989) Morphological and microtectonic evidence for a major active right-lateral strike-slip fault across central Ecuador (South America). *Annales Tectonicae* **3,** 125–139.

Wolters B. (1986) Seismicity and tectonics of Southern Central America and adjacent regions with special attention to the surrounding of Panama. *Tectonophysics* **128,** 21–46.

Woodward & Clyde Consultant, S. Francisco, CA, U.S.A. (1981) Investigaciones para los estudios del riesgo sismico del sitio de la presa Agoyan. Tech. Rep. for the Agoyan Dam Project, INECEL, Quito.

Zeil W. (1979) *The Andes, a Geological Review*. Gebruder Borntraeger, Berlin-Stuttgart, Germany.